

Soft EPMs: Design and Fabrication of a Soft Magnetic Materials for Application in Soft Actuators

A senior Design Project Submitted in Partial Fulfillment of the Requirements for the Degree
of Bachelor of Science at Harvard University

Billy Koech

S.B. Degree Candidate in Electrical Engineering

Faculty Advisors: Prof. Radhika Nagpal, Dr. Bahar Haghighat

Harvard University School of Engineering and Applied Sciences

Cambridge MA

March 1, 2020

Table of Contents

<i>I. Introduction</i>	5
A. Problem Statement	5
B. Stakeholders	5
<i>II. Background Research</i>	6
A. Literature Review	6
<i>III. Design Goals and Technical Specifications</i>	6
A. Goals	6
B. Device Size/Scale	7
C. Holding Force	7
D. Soft Iron End Permeability	7
E. Soft Iron End Compliance	7
F. Hard Permanent Magnet Coercivity	8
G. Hard Permanent Magnet Compliance	8
H. Semi-hard Permanent Magnet Coercivity	8
I. Semi-hard Permanent Magnet Compliance	8
J. Coil Conductivity	8
K. Coil Magnetic field strength (H)	8
L. Coil transient current limit	9
<i>IV. Technical Design Approach</i>	9
A. Latch Flexibility alternatives:	9
B. Soft Iron End Design: Permeability-Flexibility trade off	9
C. Soft coil Design: Current-Turns trade off	10
D. Flexible permanent magnet design: Force flexibility trade off	12
<i>V. building/Prototyping</i>	13
A. Soft Iron end prototype	13
B. Soft Coil prototype	15
C. Magnetic core prototype	16
<i>VI. Evaluation/ Verification</i>	17
A. Soft Iron Ends Verification	17
B. Soft Coil Measurements and Verification	19
C. Soft magnetic core Measurement and Verification	20
D. Assembled device Measurement and Verificaiton	20
<i>VII. Budget</i>	21
<i>VIII. Conclusion and Future work</i>	21

A.	Summary of Achieved Technical Specifications	21
B.	Future Work	21

Table of figures

Fig. 1.	Stakeholder map. SSR: Self Organizing Systems Research	5
Fig. 2.	System diagram showing the where soft Electropermanent magnet (EPM) actuators reside in a larger system. 6	
Fig. 3.	Rigid version of an Electropermanent Magnet [4].....	6
Fig. 4.	Coil and RLC meter for characterizing the soft iron ends	10
Fig. 5.	CAD of the soft iron end showing its cylindrical shape	10
Fig. 6.	Fabrication of a soft version of soft iron ends. The aim is to optimize for permeability and the tradeoff is flexibility	10
Fig. 7.	CAD of the flexible soft coil with 30 turns and 10 mm diameter	10
Fig. 8.	The aim is to decrease the number of turns and the tradeoff is the amount of current. Additionally, the conductivity of the wire limits the maximum amount of current that can flow through the wire without damaging it. 11	
Fig. 9.	Circuit schematic and simulation of current flowing through an EGaIn coil of 4 Ohms and 2 uH.....	11
Fig. 10.	Simulation results for the voltage across an EGaIn coil of 4Ohms and 2 uH. The red line represents the V _{gs} of the nMOS used to as a switch for discharging the capacitors on the coil. V _{coil} is the voltage across the coil (modelled as a resistor and an inductor) when the transistor is turned on and the capacitor discharges.	12
Fig. 11.	(a) Flexible NdFeB magnet (b) Flexible AlNiCo Magnet.....	12
Fig. 12.	Flexible NdFeB and AlNiCo placed adjacent to each other.....	12
Fig. 13.	Permanent magnet composed of ecoflex, AlNiCo and NdFeB particles	12
Fig. 14.	When fabricating the flexible magnetic cores, the aim is to optimize for magnetic force and the tradeoff is flexibility. The volume ratio of the particles in the mixture is directly proportional exerted force but inversely proportional to the flexibility.	13
Fig. 15.	Images of ferroelastomer sample #20 from appendix ### showing the top view and side view of the samples. The ruler is included for scale.	13
Fig. 16.	ARE-310 Thinky mixer configured to mix the mixtures of iron particles and ecoflex at 2000 rpm for 30 seconds.	13
Fig. 17.	CAD of mold used to fabricate ferroelastomer samples. The holes were cylindrically designed so as to fit a coil that will be used to characterize the permeability of the sample.....	13
Fig. 18.	Elcometer 4340 Automatic Film Applicator is used to create a thin layer of ecoflex that is then used to make a shell to contain iron particles.	14
Fig. 19.	CAD of particle in a shell mold.....	14
Fig. 20.	Extracting a thin ecoflex film of about 20mm by 80mm	14
Fig. 21.	Ecoflex film layed on the inner surface of one half of the mold	14
Fig. 22.	Pouring some ecoflex 30 into the assembled mold to seal one end of the mold	14
Fig. 23.	Pouring iron particles into the mold and sealing the top with ecoflex	15
Fig. 24.	Mold sealed with ecoflex 30 and place in a vacuum chamber to evict the air. The bubbles observed are due to bubbles escaping from the inside of the shell. Note that the ecoflex at the top is yet to cure.....	15
Fig. 25.	Two shells joined with “wings”	15
Fig. 26.	Tools used to separated the cojoined shells	15
Fig. 27.	Fabrication procedure for flexible coil[8]. A) Ecoflex rolled on a flat surface. B) Micro rod rolled on ecoflex surface. C) Placing coated rod on a hot plate to cure the ecoflex. D) Removal of the carbon rod and injection of EGaIn so as to make the tube conductive. Electrodes are inserted at the ends to provide electrical contact points. E) Roll tube into coil F) Embedding coil in a silicon layer.	16
Fig. 28.	Injecting EGaIn into a silicone tube using a syringe.....	16
Fig. 29.	CAD of Mold for winding coil(left) and a 3D printed version(right)	16
Fig. 30.	Coil prototype I (left) and III(right).....	16
Fig. 31.	Coil prototype IV	16
Fig. 32.	A hallbach array is used to create a homogenous magnetic field to prevent the magnetic particle from clustering or drifting.....	17

Fig. 33.	Mold for fabricating the separate bar prototype. The mixture of magnetic particles and ecoflex is poured into the holes.	17
Fig. 34.	Mold for fabricating the integrated bar prototype	17
Fig. 35.	Effect of increasing the percentage of iron on the inductance of the sample. The volume ratio refers to absolute volume ratio of iron. The blue line at the very top corresponds to the values of a shell filled with just iron filings. The red line at the bottom corresponds to the values of the coil with no core (ie. air core). Error bars are derived from the standard deviation.	17
Fig. 36.	Effect of increasing the percentage of iron on the inductance of the sample. The volume ratio refers to absolute volume ratio of iron. The blue line at the very top corresponds to the values of a shell filled with just iron filings. The red line at the bottom corresponds to the values of the coil with no core (ie. air core). Error bars are derived from the standard deviation.	18
Fig. 37.	Effect of increasing the percentage of iron by mass on the inductance. The mass ratio refers to absolute mass ratio of iron. Error bars are derived from the standard deviation.	18
Fig. 38.	Effect of increasing the percentage of iron by mass on the relative permeability. The mass ratio refers to absolute mass ratio of iron. Error bars are derived from the standard deviation.	18
Fig. 39.	Effect of vacuuming samples on the relative permeability of 300-micron particle samples. Plotted against absolute volume ratio of particles.	18
Fig. 40.	Effect of vacuuming samples on the relative permeability of 300-micron particle samples. Plotted against absolute mass ratio of particles.	19
Fig. 41.	Discharging capacitors on a coil model with 4 Ohms resistance and 2uH inductance. V(nmos) is the voltage of a signal used to switch a transistor connecting the coil to two 220uF capacitors.	20
Fig. 42.	Plot of magnetic flux of coil against amount of current flowing through the prototype IV coil.	20
Fig. 43.	Setup for measuring the magnetic flux and magnetic field strength of the flexible coil.	20
Fig. 44.	Plot of resistance of EGaIn tube conductor measured after driving a transient current across the conductor.	20
Fig. 45.	Plot of the residual magnetic field of flexible AlNiCo (left) and flexible NdFeB (right) for the separate bar prototype.	20
Fig. 46.	Plot of the residual magnetic field of the singular integrated bar prototype	20

Soft EPMs: Design and Fabrication of Soft Magnetic Materials for Application in Soft Actuators

Billy Koech
Electrical Engineering

Harvard School of Engineering
and Applied Sciences

Cambridge, MA United States of
America

bkoech@college.harvard.edu

Abstract— This project proposes that the energy efficiency of electro permanent magnets (EPMs) can be leveraged to create an actuator with less energy costs (compared to standard electromagnetic methods) and with higher compatibility for soft robotics. This actuator can be used to aid motion (moving robot subcomponents around) and control (as an actuator acting on the environment) in soft robotics. The project entails designing and building soft EPMs by fabricating soft subcomponents of EPMs that hold similar electro-magnetic properties to those the components of rigid EPMs. Such properties include a holding force of 2 Newtons for a 10-millimeter scale device. In addition to this the soft version offers higher compliance (flexibility) which enables it to be able to adapt to surfaces that the rigid EPM cannot. Measurement of the soft EPM dimensions, compliance and magnetic properties are taken to characterize it's performance compared to a rigid one and to validate the feasibility of a soft EPM.

Keywords—*Electropermanent magnet, permeability, coercivity, Ecoflex, compliance, coercivity, holding force, bistable,*

I. INTRODUCTION

Soft robotics is an emerging field with application in domains ranging from the medical industry to the food processing industry. The aim of this project is to design and build an actuator that is compatible with soft robots and has less energy costs in comparison to current common methods. Traditional methods for implementing soft actuators include pneumatic, shape memory alloys, dielectric-electro activated polymers and magnetic/electromagnetic methods. Of these methods, the most common ones are pneumatic[1] and electromagnetic methods. However, pneumatic methods require additional extensive pressure networks[2] for higher precision control[3], while most electromagnetic methods exist in rigid form[4] and require constant currents to maintain their magnetic field[5]. The cost for manufacturing and power increases for the former and latter methods respectively.

Therefore, there is a need for a soft actuator system that allows for high precision control at lower energy costs. This is the motivation of this project: to push the limit of compliance in energy efficient electromagnetic actuators.

A. Problem Statement.

Pneumatic and electromagnetic methods are the most common methods of actuation in the field of soft robotics, however, pneumatic methods require extensive pressure networks in order to achieve high precision control, while electromagnetic methods require constant current flow in order to maintain the magnetic field.

B. Stakeholders

Pushing the limit of Compliance: While soft robotics has applications in the medical and industrial domains, the exact specification and needs in these fields vary but there is always need for high precision, reliable performance and higher compliance. The wider soft actuator research community will benefit from this design because the empirical studies here will show the limits to which compliance can be pushed in EPM actuators.

The target client for this project (more specifically) is Self Organizing Systems Research(SSR) Group. Researchers in this group are always looking for methods of building systems that can self-assemble to fulfil larger tasks that could not be completed by individual agents. The actuator developed in this project would essentially enable a system of multiple agent to latch onto one another once the actuators have been embedded in the design. Below is a map showing the key stakeholders:

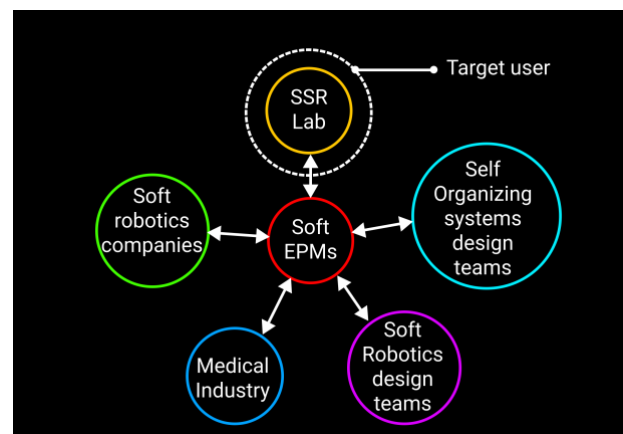


Fig. 1. Stakeholder map. SSR: Self Organizing Systems Research

The diagram below shows where the project exists as part of larger robotic system:

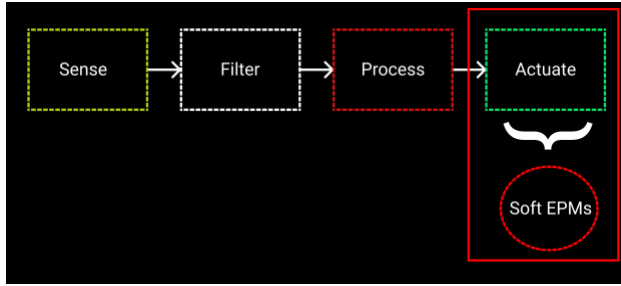


Fig. 2. System diagram showing the where soft Electropermanent magnet (EPM) actuators reside in a larger system.

II. BACKGROUND RESEARCH

A. Literature Review

The rigid version of an EPM shown in Fig. 3 is explored in depth by Knain[4] in their doctorate thesis on programmable matter. A similar explanation is used below to describe the theory of operation of this device:

Theory of operation of EPMs: This section is dedicated to explaining how rigid EPMs work, and the constraints of fabricating a soft version of it. The diagram below shows a rigid EPM:

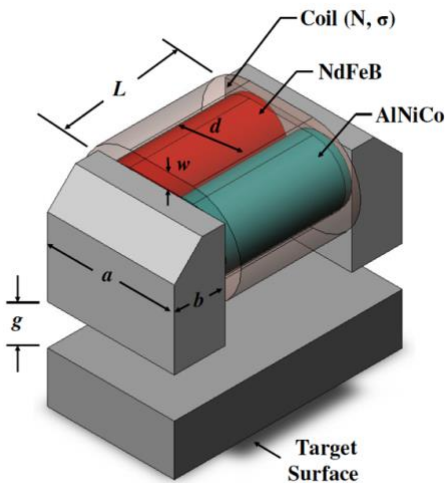


Fig. 3. Rigid version of an Electropermanent Magnet [4]

The EPM in Fig. 3 consists of 5 mains sub-components:

- Soft iron ends

- Semi hard magnet (AlNiCo)
- Hard magnet (NdFeB)
- Coil
- Target surface

The coil is wrapped around the hard-magnetic material (NdFeB) and a semi-hard magnetic material (AlNiCo) and the ends are capped with soft iron bars. A current pulse in one direction magnetizes the semi-hard magnet; A pulse in the reverse direction reverses the polarity of the semi-hard magnet. If two adjacent poles are in the same direction, then the two poles repel and all the magnetic flux is guided by the iron ends and flows through target surface in order to complete the loop. This provides the magnetic force that binds the target surface to the EPM. This is the ON state. If the adjacent poles are in opposite directions, then they attract and all the flux flows through the soft iron ends therefore closing the loop through the soft iron ends. The target surface is not attracted to the EPM. This is the OFF state.

Design and fabrication of a completely soft version of an EPM with the same number of components as the rigid EPMs has not been explored in published literature at the time that this has been written. However, there have been attempts by separate researchers to build components that resemble those of EPMs. This project aggregates their findings in the design of a fully soft EPM.

Fabrication of a soft version of an EPM has been attempted by some researchers at the Ecole polytechnique fédérale de Lausanne (EPFL) research institute[6]. Their method involves making just a flexible magnetic core. This project builds on their work but at the same time differs from theirs because all parts of the EPM in this project are converted to a soft component; not just the magnetic core.

The design of the magnetizer and switching circuit in this project is based of Knaian[4] and Haghighat's[7] designs of rigid EPMs. The same concepts on the electrical properties of a rigid copper wire are applied to derive the circuit requirements and electrical properties of a flexible coil.

The design of the flexible coil is based on that of Do et al.[8] where they fabricate an electromagnetic coil out a conductive liquid metal alloy and silicone tubes.

III. DESIGN GOALS AND TECHNICAL SPECIFICATIONS

A. Goals

The goal of this project is to fabricate a soft electropermanent magnet actuator to aid motion and control in soft robotics. The actuator should have a length of about 1cm and exert about 2 Netwons of holding force when latched. These specifications along with others are explained in detail in this section: Below are the fabrication sub-goals:

¹ "Soft" refers to the magnetic property as opposed to the compliance

1. Fabricate soft version of iron poles with sufficient permeability.
2. Fabricate soft version of semi-hard magnet (AlNiCo) with sufficient magnetic remanence.
3. Fabricate soft version of hard magnet (NdFeB) with equivalent remanence to that of the fabricated AlNiCo.
4. Fabricate a soft coil.
5. Assemble the EPM latch.
6. Characterize soft EPM and compare performance to a rigid version of the similar size.

B. Device Size/Scale

- **Quantitative Description:** Length of 1cm or less.
- **Justification:** Previous versions of EPMs, developed by other researchers, have been able to attain lengths of 0.5mm[4] and 1cm[7]. This project will aim to replicate their designs but out of soft materials.
- **Measurement:** Length can be measured with a ruler.

C. Holding Force

- **Quantitative Description:** The aim is to achieve a holding force that is as close as possible to that of an equivalent rigid EPM. This project's target saturation Force is 2N.
- **Justification:** One paper shows that an EPM of size 0.5mm could achieve a saturation force of 4.4N [4]. Saturation force is the force maximum force that can be exerted by an electromagnet. An increase in applied external magnetic field cannot increase the magnetization of the material any further. Another shows that two EPMs of size 1cm attracting each other could achieve a holding force of 1.24N[7]
- **Measurement:** Holding force can be measured by attaching the soft EPM to a spring of known spring constant k and measuring the extension of the spring until the EPM detaches from the target surface. The force can be computed using the formula below:

$$F = -k \times x \quad \text{Equation 1}$$

Where

F – holding force
 k – spring constant
 x – extension

D. Soft Iron End Permeability

- **Quantitative Description:** Relative permeability equal to or greater than 10.
- **Justification:** The relative permeability of iron powder ranges between 14 and 100 [9]. A guide on soft magnetic material by Wulf Günther and Paul Winkler suggests that if the permeability is less than 500 then the flux begins to stray.[10]: “In case of low materials permeability (<500) or gaps or certain core / winding designs, where the field and the flux is not guided by the magnetic material completely, the field and flux parts through air...”[10] The implications of this on the EPM iron ends is uncertain.
- **Measurement:** Permeability can be calculated from the inductance of a material. Inductance can be measured by placing a coil of known turns N around a material and connecting the coil to an RLC meter.

$$L = \frac{\mu N^2 A}{l} \quad \text{Equation 2}$$

Where:

L – inductance

μ_o – absolute magnetic permeability

N – number of turns

A – cross sectional area of coil

l – length of coil

E. Soft Iron End Compliance

- **Quantitative Description:** The target range for compliance is between 0.001 and 0.05 GPa (Young's Modulus)
- **Justification:** Compliance is dependent on the substrate material used as a continuum medium for the particles. It is projected that the addition of soft iron particles decreases the compliance, but the reported values for ferro-elastomer mixtures is between 0.001 and 0.05 GPa[3].
- **Measurement:** Young's modulus can be measured by setting up an experiment to measure stress and strain[11]. The equation below shows the definition of young's modulus:

$$E = \frac{F/A}{\Delta L/L} \quad \text{Equation 3}$$

Where:

E - Young's modulus

F - Force exerted

A - Area

ΔL - Change in length

L - Initial length

F. Hard Permanent Magnet Coercivity

- **Quantitative Description:** Coercivity is a measure a materials resistance to magnetization or demagnetization. The target coercivity for the hard-permanent magnets is about 1000kA/m
- **Justification:** NdFeB is used in the implementation of the rigid EPM[4]. It's coercivity is about 1000 kA/m[12].
- **Measurement:** Coercivity of a material can be measured using a magnetometer. It can also be calculated from the B-H graph of the magnetic material.

G. Hard Permanent Magnet Compliance

- **Quantitative Description:** The target range for compliance is between 0.001 and 0.05 GPa; this is similar to that of the soft iron ends.
- **Justification:** Reported values for ferro-elastomer mixtures is between 0.001 and 0.05 GPa[3].
- **Measurement:** Compliance can be measured by calculating Young's modulus. Refer to Equation 3.

H. Semi-hard Permanent Magnet Coercivity

- **Quantitative Description:** Coercivity of 50 kA/m.
- **Justification:** AlNiCo is used in the implementation of the rigid EPM[4]. It's coercivity of AlNiCo V is about 50 kA/m [13].
- **Measurement:** Coercivity of a material can be measured using a magnetometer. It can also be calculated from the B-H graph of the magnetic material.

I. Semi-hard Permanent Magnet Compliance

- **Quantitative Description:** The target range for compliance is between 0.001 and 0.05 GPa; this is similar to that of the soft iron ends.
- **Justification:** Reported values for ferro-elastomer mixtures is between 0.001 and 0.05 GPa[3].
- **Measurement:** Compliance can be measured by calculating Young's modulus. Refer to Equation 3.

J. Coil Conductivity

- **Quantitative Description:** The limit on the amount of current is determined by the properties of the conductive material used to make the coil. This project uses Eutectic Gallium Indium (EGaIn) which is a conductive liquid metal alloy that can be injected or embedded in a channels. The literature value for its conductivity is $\sigma = 3.4 \times 10^6 \text{ Sm}^{-1}$ [14]. This value together with the dimension of the wire and the chemical properties of the liquid metal alloy(EGaIn) will used to determine the amount of current that can be driven through the wires without damaging the wire.
- **Justification:** Various researchers have attempted to make soft coils out of EGaIn and they have reported conductivity within similar of magnitude as $\sigma = 3.4 \times 10^6 \text{ Sm}^{-1}$. [11]–[13]
- **Measurement:** Conductivity is the reciprocal of resistivity. Resistivity can be calculated from the resistance of a material (measured using an ohmmeter), the cross-sectional area and the length of the conductor:

$$\rho = R \frac{A}{L} \quad \text{Equation 4}$$

Where:

ρ - resistivity

R – resistance

A - Area

L - Length

$$\sigma = \frac{1}{\rho} \quad \text{Equation 5}$$

Where:

ρ - resistivity

σ – conductivity

K. Coil Magnetic field strength (H)

- **Quantitative Description:** Magnetic field of 100 kA/m
- **Justification:** The material used for the semi-hard permanent magnet (AlNiCo) has a coercivity of 50kA/m. In order to reverse its polarity the magnetic field of the coil has to be equivalent to amagnitude of 100kA/m; the first 50kA/m will demagnetize AlNiCo and the additional 50kA/m will magnetize it in the opposite direction.
- **Measurement:** Magnetic field strength(H) can be derived from magnetic field(B) as shown in the equation below. Magnetic field (B) can be measured with a Gauss meter:

$$H = \frac{B}{\mu} \quad \text{Equation 6}$$

Where:

H – magnetic field strength

μ - absolute magnetic permeability

B – magnetic field

L. Coil transient current limit

- **Quantitative Description:** The coil should be able to support about 20A for the purpose of generating a magnetic field that can reverse the polarity of the semi-hard permanent magnet.
- **Justification:** In one publication the researchers used a RLC circuit to drive 22A of current through a 32-turn coil made out of 26 AWG in order to reverse the polarity of the AlNiCo magnet[7].
- **Measurement:** Transient currents can be measured with an oscilloscope that has a current probe.

TABLE I. SUMMARY OF TECHNICAL SPECIFICATIONS

Specification	Target value
Device Scale	1 cm long
Holding Force	2 N
Soft Iron End relative permeability	10
Soft Iron End compliance	0.001 to 0.05 GPa
Hard Permanent Magnet coercivity	1000 kA/m
Semi-hard Permanent coercivity	50 kA/m
Semi-hard Permanent magnet compliance	0.001 to 0.05 GPa
Coil conductivity	$3.4 \times 10^6 \text{ Sm}^{-1}$
Coil magnetic field strength	100 kA/m
Coil transient current limit	20 A

IV. TECHNICAL DESIGN APPROACH

As shown in section III, a soft EPM consists of 5 different component each with their own specifications. Given that none of these subcomponents are available commercially (or in prefabricated form), they have to be designed and fabricated from raw materials. There is a reason for the apparent absence of literature or research on building a fully flexible EPM: converting each component to

is a large feat on its own therefore the project is split into three alternatives in order of increasing total flexibility. The term “latch” in the sections that follow is used to refer to a fully assembled device.

A. Latch Flexibility alternatives:

- **Flexible Iron Ends :** This alternative entails just converting the iron ends into flexible form but leaving every other component in rigid form. The soft iron ends are the main point of contact between the target surface and the latch therefore flexible iron ends might be sufficient to allow the device to adapt to surfaces.
- **Flexible Iron ends and Coil:** This alternative involves converting the iron ends and the coil to flexible form. The permanent magnets retain their rigid form.
- **Fully Flexible device:** This alternative entails converting the iron ends, coil and permanent magnets into flexible form. In theory such a device would have the highest possible compliance in comparison to the other alternatives.

TABLE II. COMPARISON OF ALTERNATIVES

Alternative	Advantage	Potential constraints/Disadvantages
Flexible Iron End	The soft iron ends are the main point of contact therefore the device can adapt to rigid planar surfaces and some non-planar surfaces	Compliance is limited to just one component. Difficult to latch onto highly irregular target surfaces
Flexible Iron ends and coils	More compliance in comparison to the previous alternative	The additional compliance is still impeded by the rigid permanent magnets around which the coil is wound
Fully flexible device	Maximum attainable compliance would allow the full device to adapt to irregular non-planar target surfaces	Acquiring magnetic particles and fabricating with magnetized particles is industrially challenging and would require specialized equipment such as a hallbach array and a ball mill.

The objective of this project is it push the limit of compliance therefore The third alternative is pursued despite the evident challenges of acquiring materials and fabrication. That’s not all: Given the sequential nature of the three alternatives, the other two alternatives are also pursued as milestones towards the achievement of a fully soft EPM.

B. Soft Iron End Design: Permeability-Flexibility trade off

Geometry Design: In order for the iron ends to be characterizable they have to be able to fit a coil of 10 millimeters diameter and 200 turns which is used to measure

the inductance of the flexible iron end sample as shown in Fig. 4.



Fig. 4. Coil and RLC meter for characterizing the soft iron ends

This method of characterization therefore drove the design for the shape of the iron end as shown below.

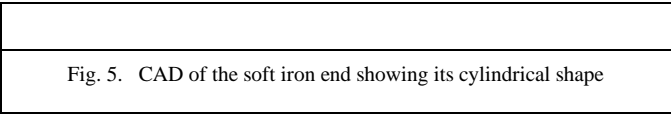


Fig. 5. CAD of the soft iron end showing its cylindrical shape

Design for flexibility: Fabrication of a flexible iron ends involves combining iron particles with an elastomer in order to attain flexibility while preserving the high permeability property of iron. Two fabrication processes are designed both of which are discussed in the prototyping section. The first alternative is mixing iron particles with an elastomer. The second involves creating an elastomeric shell into which particles can be embedded; the latter attains flexibility because the particles in a shell can move and adapt to any shape.

Both of these methods have an associated *permeability-flexibility trade off*: The volume ratio of iron in the mixture is proportional to the permeability and inversely proportional to the flexibility. The size of the particles also factors into the permeability and this relationship is discussed in the measurement/verification section. Fig. 6 summaries the factors at play in the fabrication of the flexible iron ends:

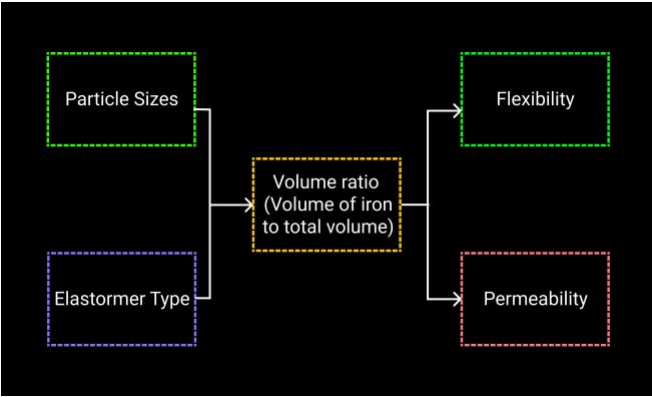


Fig. 6. Fabrication of a soft version of soft iron ends. The aim is to optimize for permeability and the tradeoff is flexibility

C. Soft coil Design: Current-Turns trade off

Geometry Design: The coil should be able to wrap around the permanent magnet cores with enough turns to generate a magnetic force H of 100kA/m. The design below shows a coil of 30 turns and 10 millimeters diameter. This is number is subject to change based on the first prototype from which actual values of resistivity and inductance of the coil can be determined.

The geometry of the coil is similar to that of a cylindrical solenoid as shown in the Figure below:

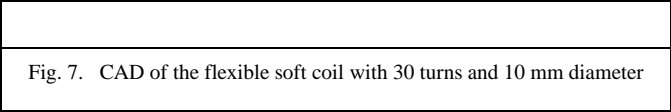


Fig. 7. CAD of the flexible soft coil with 30 turns and 10 mm diameter

Design for flexibility: Copper wire is already flexible but once wound into turns it becomes inflexible. This necessitates the need for a more flexible coil: the coil design involves a flexible tube into which conductive liquid metal alloy is injected. Three alternatives are developed and explored in the prototyping section: the first involves injecting Eutectic Gallium Indium(EGaIn) into a self-fabricated or purchased silicon tube[8]. The second involves mixing silver nano wires with an elastomer in order to attain a conductive elastomeric wire. The fabrication procedure for each of these alternatives is discussed in the prototyping section.

The objective while fabricating the coil is to decrease the number of turns so as to meet the size specification while not compromising on the amount of magnetic force generated; the trade of for decreasing the turns is increase in the amount of current needed to generate an equivalent magnetic flux as shown in *Equation 7*:

$$B = \mu N I \quad \text{Equation 7}$$

Where:

B - Magnetic field

μ - absolute

permeability

N - number of turns

I - amount of
current

$$R = \frac{\rho \ell}{A} \quad \text{Equation 8}$$

Where:

R - resistance

ℓ - length of wire

ρ - resistivity of

EGaIn

A - cross sectional
area of wire

The amount of current that can be passed through the wire also has a limit defined by the resistance of the wire and its inductive property when wound into a coil; high currents generally have the tendency to burning (fuse) wires due to energy dissipation in the form of I^2R losses. The relationships discussed above are summarized in the diagram below:

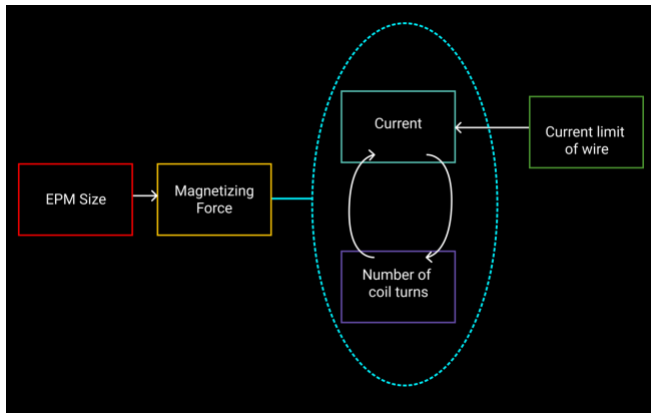


Fig. 8. The aim is to decrease the number of turns and the tradeoff is the amount of current. Additionally, the conductivity of the wire limits the maximum amount of current that can flow through the wire without damaging it.

Design to support a transient current: Generation of the magnetic flux needed to reverse the polarity of AlNiCo will be through pulse magnetization where a capacitor is discharged on the coil to generate a high transient current. This project borrows from a design by other researchers where they attained 30A for 50 microseconds[7].

The coil can be modelled as an RL component where the resistance is determined by the conductivity of EGaIn, its length and cross-sectional area as shown in equation Equation 8; the inductance can be determined from the permeability of the core, the number of turns, the length, and the cross section of the coil as shown in Equation 9.

A combination of the coil model and a circuit for generating the current needed to create a magnetic field is shown in Fig. 9.

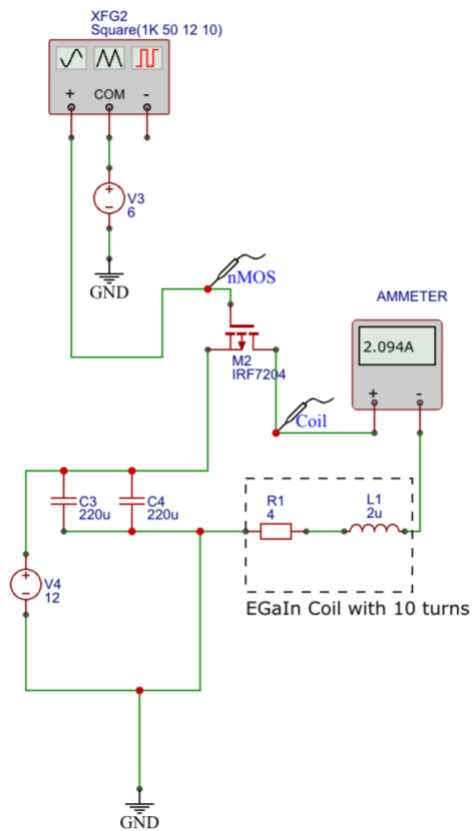


Fig. 9. Circuit schematic and simulation of current flowing through an EGaIn coil of 4 Ohms and 2 uH

Based on the above schematic a simulation of a conductive coil with a resistance 4 Ohms, inductance of 2 uH and Capacitance 400uF is conducted to arrive at the graph in Fig. 10 . The amount of current across the coil is determined to be about 2.094 A. This makes sense because the conductivity of EGaIn is one order of magnitude less than that of copper therefore an equivalent circuit that drives 20A of current

through a copper wire of a given length and cross section should drive about 2A over the same length and cross section of EGaIn.

$$L = \frac{\mu N^2 A}{\ell} \quad \text{Equation 9}$$

Where:

L - inductance

ℓ - length of coil

N – number of turns

A – cross sectional area of coil (not wire)

μ – permeability of core

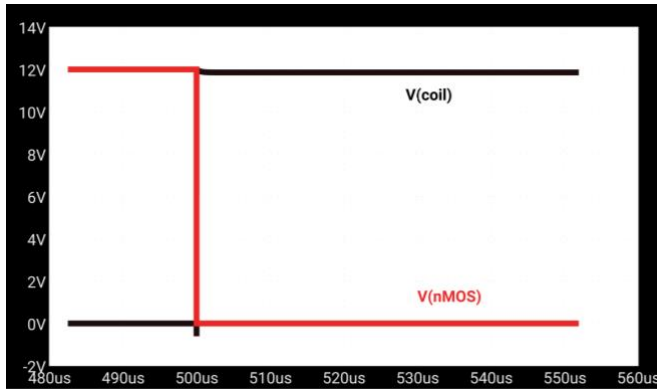


Fig. 10. Simulation results for the voltage across an EGaIn coil of 40hms and 2 uH. The red line represents the Vgs of the nMOS used to as a switch for discharging the capacitors on the coil. V coil is the voltage across the coil (modelled as a resistor and an inductor) when the transistor is turned on and the capacitor discharges.

With this amount of current the approximate amount of turns needed to generate a magnetic force H of 100kA/m is about 500 in accordance with Equation 10. This number of turn can be further reduced by increasing the diameter of the EGaIn wire to decrease the total resistance. (#Double the diameter to decrease resistance by a factor of 2 thereby decreasing the turns by a factor of 2)

$$N = \frac{H_{AlNiCo} \ell_{coil}}{I_{circuit}} \quad \text{Equation 10}$$

D. Flexible permanent magnet design: Force flexibility trade off

Geometry design: Two alternatives are ideated for the geometry of the permanent magnets. The first resembles the rigid version of the EPM where each permanent magnet is fabricated with from a mixture of magnetic particles and an elastomer then molded into a cylinder. In this design each permanent magnet exists as a separate cylinder from the other, but they are placed adjacent to each other in the final assembly. Fig. 11 and Fig. 12 show the CAD for the first permanent magnets prototype design.

Fig. 11. (a) Flexible NdFeB magnet (b) Flexible AlNiCo Magnet

Fig. 12. Flexible NdFeB and AlNiCo placed adjacent to each other.

The second design (shown in Fig. 13) involves mixing both magnetic particles (NdFeB and AlNiCo) with an elastomer to create one homogenous mixture. The mixture would then be cured in a mold to arrive at a geometry shown in Fig. 13. The edges are curved to ensure that a coil wrapped around it is in flush with the surface. Some researchers at EPFL attempted to create such a magnet by mixing NdFeB and AlNiCo particles with an elastomer [6]. They recommended using $5 \mu m$ grain size for NdFeB and $5 \mu m$ for AlNiCo to yield a high filling factor [6]. This design follows those recommendations.

Fig. 13. Permanent magnet composed of ecoflex, AlNiCo and NdFeB particles

Design for flexibility: Unlike the soft iron ends, magnetic particles cannot be fabricated using the particles in a shell method because the individual particles would be free to move in the shell; that is, an applied magnetic field would change the orientation of the particles rather than change their polarity. For this reason, only one design is proposed: Mixing the particles with an elastomer to create a homogenous mixture. Once such a mixture has cured the particles will not be able to change their orientation but the sample as whole should be able to bend thereby achieving flexibility. The volume ratio of the magnetic particles in the mixture is proportional to the magnetic force and inversely proportional to the flexibility; this is the trade off when designing the magnetic cores and is summarized in the illustration in Fig. 14.

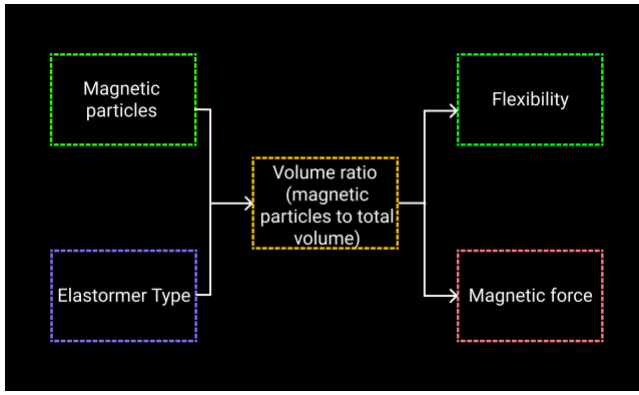


Fig. 14. When fabricating the flexible magnetic cores, the aim is to optimize for magnetic force and the tradeoff is flexibility. The volume ratio of the particles in the mixture is directly proportional exerted force but inversely proportional to the flexibility.

V. BUILDING/PROTOTYPING

A. Soft Iron end prototype

Two alternatives for designing the soft iron ends are ideated in the design section: First, mixing iron particles of different sizes with an elastomer (*ferroelastomer* alternative); and second, enclosing particles in a shell (*particle in a shell* alternative). Both alternatives are explored and the best of the two chosen. The results show that the particles in a shell alternative have higher permeability than a ferroelastomer alternative for samples fabricated with the same grain sizes. However the fabrication procedure for the ferroelastomers and the data is still included here because it presents interesting findings on the behavior of iron when mixed with an elastomer. The fabrication procedures are discussed below:

Ferroelastomer fabrication methodology: The samples are fabricated by mixing an elastomer (Ecoflex 30) with iron particles of different sizes at different mass and volume ratios. Ecoflex 30 was chosen because it offers the highest possible compliance in comparison to Ecoflex 20 and 10. Below are the particle sizes used to fabricate samples in decreasing size:

- -20 mesh (840 microns)
- -70 mesh (210 microns)
- -200 mesh (74 microns)
- 6-10microns
- 1-4 microns

The samples were fabricated by mixing iron particles with Ecoflex 30 in increasing volume ratios of iron particles. The first step starts with pouring a predetermined volume of iron particles in a plastic cup and measuring the mass. This is followed by adding Ecoflex 30 part A into the same plastic cup. An equivalent amount of Ecoflex 30 part B is then poured into the same cup. The mixture is then mixed in an ARE-310 Thinky mixer. Most of the samples are mixed at 2000 revolutions per minute (rpm) for 30 seconds as shown in Fig. 16. The samples

are then poured into a mold with holes of 10mm diameter (shown in Fig. 15 and Fig. 17) and placed in a 60°C oven for about an hour (or more for other samples). The molds were designed so as to fit the characterizing coil mentioned in the design section. A table with all the parameters used in the design of this experiment as well as the results is provided in appendix ###. Images of the sample are also available in a git repository provided in the references[15]. The measurement section discusses the implications of the measured sample permeabilities.

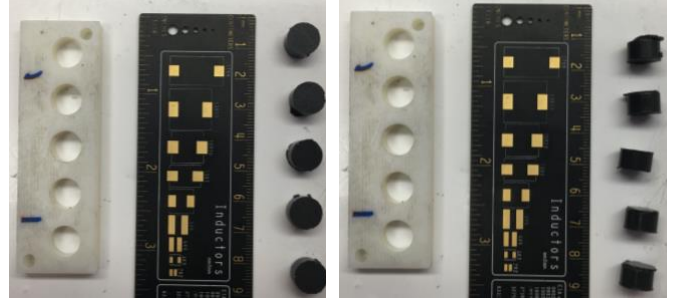


Fig. 15. Images of ferroelastomer sample #20 from appendix ### showing the top view and side view of the samples. The ruler is included for scale.



Fig. 16. ARE-310 Thinky mixer configured to mix the mixtures of iron particles and ecoflex at 2000 rpm for 30 seconds.

Fig. 17. CAD of mold used to fabricate ferroelastomer samples. The holes were cylindrically designed so as to fit a coil that will be used to characterize the permeability of the sample.

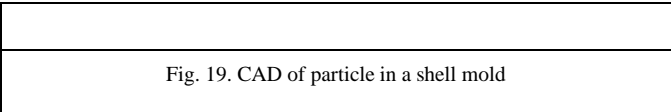
Particle in a shell fabrication methodology: The samples are fabricated by enclosing particles in an elastomeric shell. It starts with the creation of a thin layer of Ecoflex 30 using a thin film applicator (Elcometer 4340 Automatic Film

Applicator) shown in Fig. 18. The resulting film had a thickness of 0.3 millimeters.



Fig. 18. Elcometer 4340 Automatic Film Applicator is used to create a thin layer of ecoflex that is then used to make a shell to contain iron particles.

The film is then cut into strips of about 20mm by 80mm as shown in Fig. 20. These dimensions are chosen so as to fit a mold designed to create a shell out of these layers. The mold is shown in Fig. 19.



A very thin layer of Vaseline is applied onto the inner surface of these molds to prevent the Ecoflex strips from sticking onto the surfaces when demolding. The strip of Ecoflex film is then laid on the inner surface of the mold such that the strip is in flush with the curving surfaces as shown in Fig. 21. Uncured Ecoflex is then poured on the surface to act as an adhesive agent; two mirrored halves of the molds are then assembled and secured using nuts and bolts. A bottom layer for the mold is then attached and also fastened in place using nuts and bolts. Some Ecoflex is then poured from the open side of the mold. The purpose of the poured Ecoflex is to seal one end of the cylindrical shells as shown in Fig. 22.

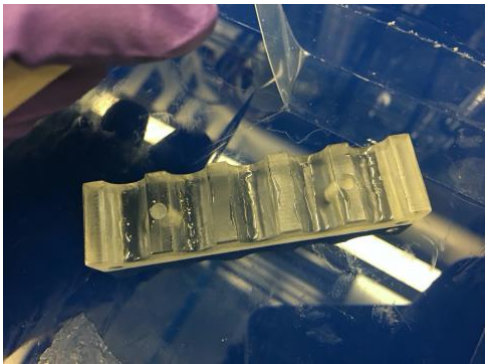


Fig. 20. Extracting a thin ecoflex film of about 20mm by 80mm



Fig. 21. Ecoflex film layed on the inner surface of one half of the mold

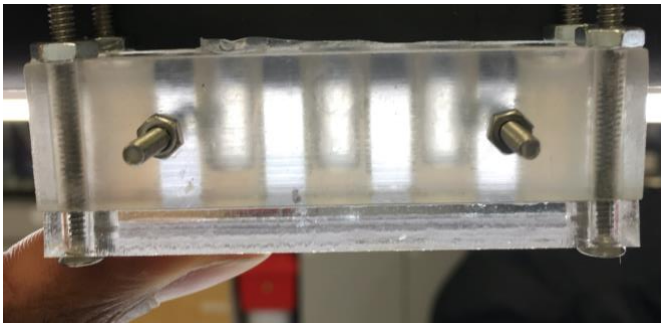


Fig. 22. Pouring some ecoflex 30 into the assembled mold to seal one end of the mold

The mold is then placed in a 60°C oven for 1 hour to cure the Ecoflex. Once it has cured, it is removed, and iron particles are poured into the holes leaving about a 3mm space at the top for sealing the shell (Fig. 23). The top is sealed by pouring ecoflex and leaving it to cure in the oven again for 1 hour. Some samples were placed in a vacuum chamber) set to 100 KPa for one hour to evict all the air inside the shell. Fig. 24 shows one such mold after it has been removed from the vacuum chamber.

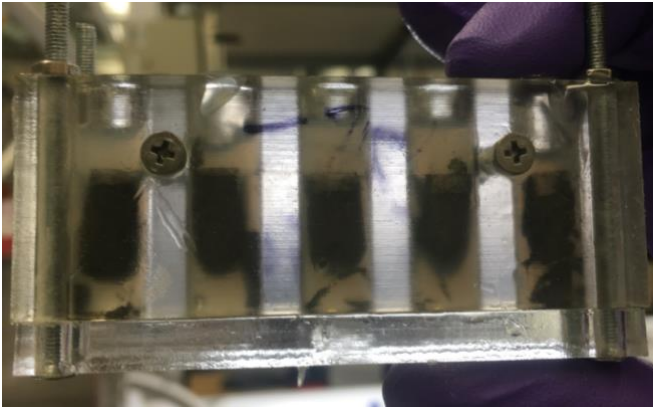


Fig. 23. Pouring iron particles into the mold and sealing the top with ecoflex



Fig. 24. Mold sealed with ecoflex 30 and place in a vacuum chamber to evict the air. The bubbles observed are due to bubbles escaping from the inside of the shell. Note that the ecoflex at the top is yet to cure.

Once the samples have cured, the mold is taken apart by opening the nuts and bolts. The different samples are then separated by cutting across the “wings” joining the samples with a scalpel:

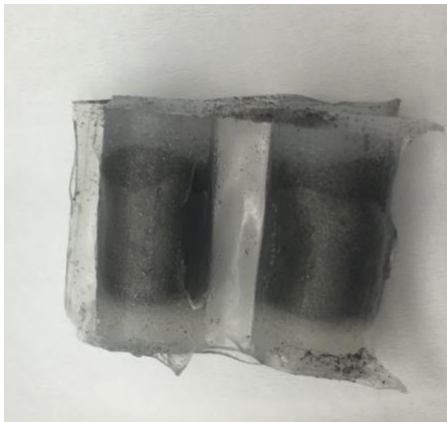


Fig. 25. Two shells joined with “wings”



Fig. 26. Tools used to separated the cojoined shells

After measuring the permeabilities of the vacuumed and non-vacuumed samples, it is noted that the non-vacuumed samples have higher permeabilities than the vacuumed ones. This is counterintuitive as one would expect tightly packed shells to have higher permeabilities. This still remains a mystery, and a discussion attempting to explain this is provided in the measurement/verify section. A full table of all the fabricated samples and the measurements for the permeabilities are provided in appendix #####.

B. Soft Coil prototype

Two major prototyping alternatives were developed in the design section. The first is creating flexible wires by mixing silver nano wires with Ecoflex. The second is creating a silicone tube by either rolling a thin film of silicone or purchasing prefabricated silicon tubes into which a conductive metal alloy can be injected. The first alternative failed as the mixture of silver nano wires and Ecoflex lost its conductivity after curing. Therefore, this section details the procedure for fabricating the functioning alternative:

Silicone tube with EGaIn fabrication methodology:

An attempt was made to create a tube from rolling a thin silicone film but it proved too difficult to seal; furthermore the achieving a thin uniform diameter was a large feat given the lack of a specialized high accuracy rolling device. Another option was to apply silicone on a carbon rod and remove the electrode after curing to remain with a tube like structure; this would be done in a fashion similar to that of Do et al.[8] in Fig. 27.

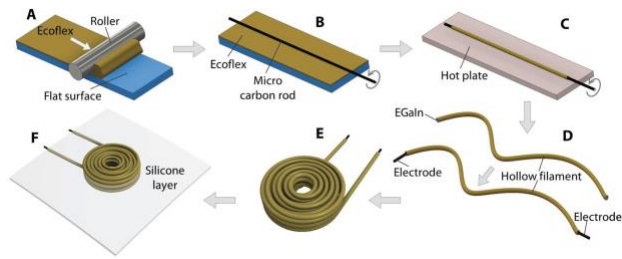


Fig. 27. Fabrication procedure for flexible coil[8]. A) Ecoflex rolled on a flat surface. B) Micro rod rolled on ecoflex surface. C) Placing coated rod on a hot plate to cure the ecoflex. D) Removal of the carbon rod and injection of EGAIn so as to make the tube conductive. Electrodes are inserted at the ends to provide electrical contact points. E) Roll tube into coil F) Embedding coil in a silicon layer.

However, this also proved to be challenging to control the thickness therefore the preferred option became purchasing prefabricated silicon tubes.

Two diameters are purchased: 0.3mm and 0.5mm inner diameters. Each tube is injected with EGAIn using a syringe (30Ga syringe for the 0.3 mm tube and 27Ga syringe for the 0.5m) as shown in Fig. 28. A copper electrode is then inserted into the tube at each end (30 AWG and 28 AWG copper for the 0.3mm tube and 22AWG for the 0.5mm tube). The 28AWG and 22AWG wires are thick enough to tightly fit into the tube therefore not requiring any additional sealant. Table VII shows the measurement results of the EGAIn Wire.



Fig. 28. Injecting EGAIn into a silicone tube using a syringe

After the wires are fabricated successfully Ecoflex 30 is poured onto the tube’s outer surface(to act as an adhesive) before winding the wire on a 3D printed cylindrical mold of 10mm diameter; for easy demolding, Vaseline is applied to the surface of the mold prior to winding.

Prototype I and III were wound successfully as shown in Fig. 30. Prototype II lost its ability to conduct due to a separation in liquid metal alloy channel. Prototype I and III prototypes also lost their conductivity due to excessive stretching of the wire when winding around the mold.

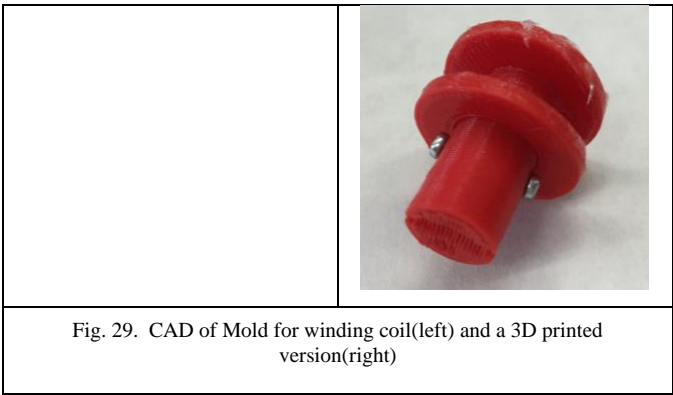


Fig. 29. CAD of Mold for winding coil(left) and a 3D printed version(right)



Fig. 30. Coil prototype I (left) and III(right)

A fourth prototype is therefore developed where the EGAIn is injected into the tube after the tube has been wound into a coil. This prototype worked better as the coil retained its conductivity. Table VIII shows the coil characteristics; Fig. 31 shows its appearance.

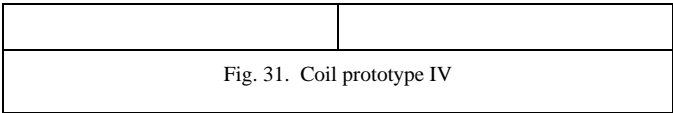


Fig. 31. Coil prototype IV

C. Magnetic core prototype

The magnetic core is fabricated by mixing magnetic particles with Ecoflex 30. Two prototyping procedures are explained below; the first prototype -*separate bar* prototype - consist of two flexible cylindrical bars (one AlNiCo and the other one NdFeB) as mentioned in the design section; the second prototype – *singular integrated bar* prototype – consists of a single bar made from mixing together AlNiCo powder and NdFeB powder.

Acquiring magnetic particles proved to be challenging as most companies do not offer the required magnetic grades for this project (shown in the Table III below) or have lead times that exceeded the time scope of this project. Given this constrain the project is likely to only attain the second milestone of device compliance whereby the every component is flexible but the permanent magnets.

TABLE III. MAGNETIC PARTICLES GRADES[13]

Material	Grade	Coercivity (kA/m)	Remanence Br (T)
NdFeB	N40	1000	1.28
AlNiCo	V	50	1.26

Separate bar fabrication methodology: The AlNiCo flexible bar sample is fabricated by mixing an Ecoflex 30 with AlNiCo particles of size $50\mu\text{m}$ at different volume ratios. The mixture is mixed in the ARE-310 Thinky mixer at 2000rpm for 30 seconds. The mixture is then placed in a hallbach array (Fig. 32) and cured in a 60°C oven. The purpose of the hallbach array is to provide a homogenous magnetic field that aligns the particles in one orientation and prevents clustering. The homogeneity of the field also prevents the particles from drifting in any direction.

Fig. 32. A hallbach array is used to create a homogenous magnetic field to prevent the magnetic particle from clustering or drifting.

Fig. 33. Mold for fabricating the separate bar prototype. The mixture of magnetic particles and ecoflex is poured into the holes.

The same procedure is repeated for the flexible NdFeB bar. The hallbach array is particularly useful while fabricating NdFeB because it has two axes of magnetization – one easy to magnetize and the other difficult to do so. The objective is to align them in the difficult axis because magnetization in this axis enables it to retain its high coercivity; this is important because in the operation of the device the polarity of the NdFeB component should never change. Once both bars have cured they are characterized using a Gauss meter and a pulse magnetizer to generate a B-H graph (Fig. 45).

Singular integrated bar fabrication methodology:

This procedure involves first mixing the AlNiCo and NdFeB particles with Ecoflex 30 at different increasing volume ratios. The composition is then mixed in a Thinky mixer at 2000rpm for 30 seconds and allowed to cure in a hallbach array placed in a 60°C oven. After curing it is also characterized using a Gauss meter and a pulse magnetizer.

Fig. 34. Mold for fabricating the integrated bar prototype

Rigid bar prototype: As the name suggests, this prototype consist of rigid bars. Therefore, these will not contribute to the total compliance of the device, but they have the advantage of being smaller and exerting greater force compared to a fabricated flexible magnet of equivalent size.

VI. EVALUATION/ VERIFICATION

A. Soft Iron Ends Verification

This section discusses the technical specifications met by the soft iron ends prototype. Of the particles used to fabricate the ferroelastomers, the 100-micron ones exhibits the highest permeabilities across the range of volume ratios. These result are used to guide the fabrication of the particles in a shell samples in that the 100-micron are the ones embedded inside the shells.

Ferroelastomer prototype characterization:

Characterization is done by connecting an RLC meter to a coil of 10mm diameter and 200 turns. Each sample is inserted into this coil and its inductance measured. The values are recorded and can be found in appendix ###.

The figures below show the permeability of the samples as a function of volume. The raw data is available at repository included in the references[15].

The graphs below suggest that the 300-micron particles have higher permeability for the same mass ratio across the different particle sizes.

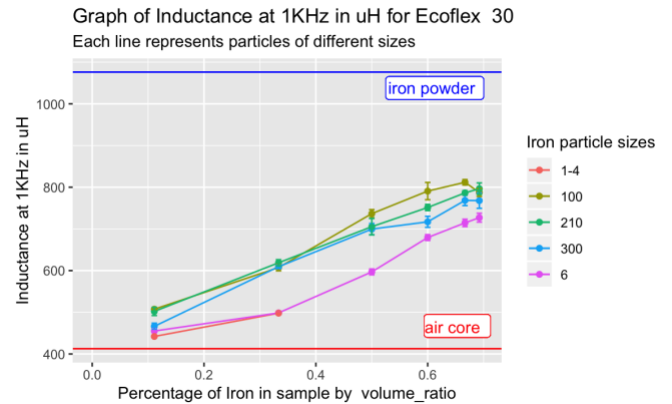


Fig. 35. Effect of increasing the percentage of iron on the inductance of the sample. The volume ratio refers to absolute volume ratio of iron. The blue line at the very top corresponds to the values of a shell filled with just iron filings. The red line at the bottom corresponds to the values of the coil with no core (ie. air core). Error bars are derived from the standard deviation.

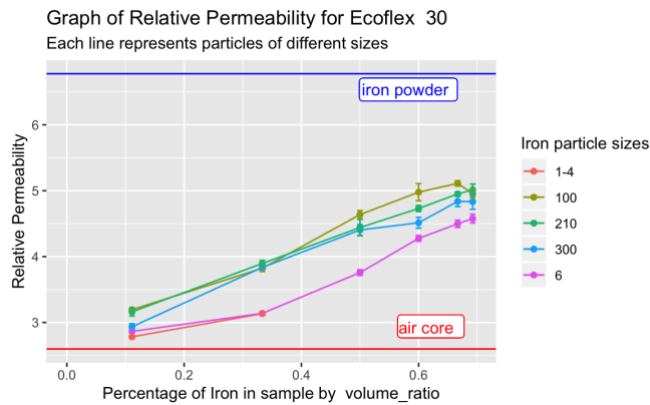


Fig. 36. Effect of increasing the percentage of iron on the inductance of the sample. The volume ratio refers to absolute volume ratio of iron. The blue line at the very top corresponds to the values of a shell filled with just iron filings. The red line at the bottom corresponds to the values of the coil with no core (ie. air core). Error bars are derived from the standard deviation.

As expected the values of inductance and permeability increase with increase in the percentage of iron. 100-micron particles exhibit the highest values of permeability for most of the volume ratios. However, the line has a dip after 0.66; at 0.69 volume ratio the permeability seems to be lower than at 0.66. A similar trend is observed for the 300-micron particles where the permeability flattens out after 0.66 volume ratio. The reason for the flattening and dipping is still not know.

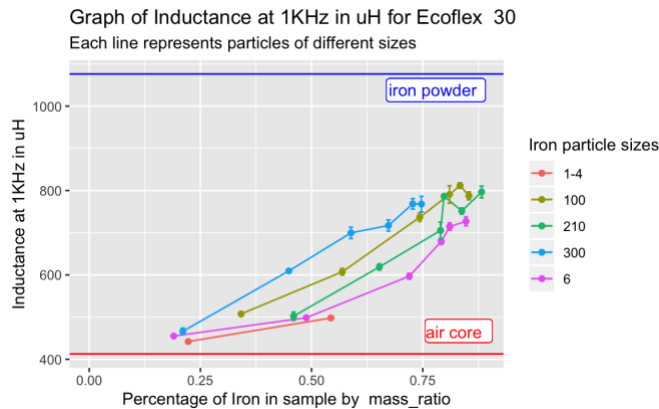


Fig. 37. Effect of increasing the percentage of iron by mass on the inductance. The mass ratio refers to absolute mass ratio of iron. Error bars are derived from the standard deviation.

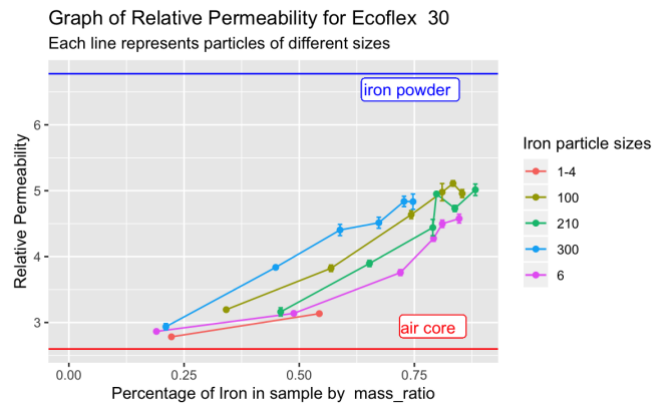


Fig. 38. Effect of increasing the percentage of iron by mass on the relative permeability. The mass ratio refers to absolute mass ratio of iron. Error bars are derived from the standard deviation.

The same data used to make the volume ratio graphs is also used in Fig. 37 and Fig. 38 to create plots of inductance and permeability against mass ratio. The misalignment of the ratio values of the graph is due to the methodology of the experiment which prioritizes volume ratio alignment over mass ratio alignment. Regardless the graphs exhibit similar general trend to that of the volume ratio where the inductance and permeability increases with increase in the ratio of iron.

Some of the ferroelastomer samples are placed in a vacuum chamber before being placed in the oven. It is observed that the permeability of the vacuumed samples is generally lower than that of the non-vacuumed samples as shown in the figure below:

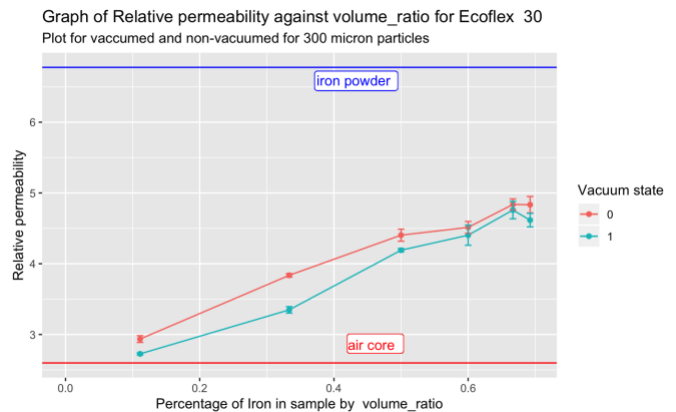


Fig. 39. Effect of vacuuming samples on the relative permeability of 300-micron particle samples. Plotted against absolute volume ratio of particles.

Graph of Relative permeability against mass_ratio for Ecoflex 30
Plot for vacuumed and non-vacuumed for 300 micron particles

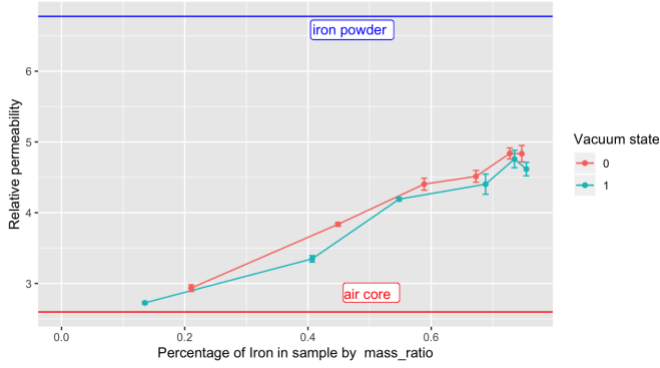


Fig. 40. Effect of vacuuming samples on the relative permeability of 300-micron particle samples. Plotted against absolute mass ratio of particles.

Particles in a shell characterization: While fabricating the shells, some samples are placed in a vacuum chamber to evict air pockets from the shell while others are not. The non-vacuumed samples exhibit higher permeability than the vacuumed samples as shown in the table below.

TABLE IV. MEASURED INDUCTUANCE OF VACUUMED AND NON-VACUUMED PARTICLE IN A SHELL SAMPLES

Particles sizes (microns)	Vacuumed?	Mean Inductance	Standard Deviation of Inductance
100	Yes	690.65	23.47
100	No	791.02	18.39

Also, it was observed that particle in a shell samples had comparable permeability to the ferroelastomer samples with the highest absolute volume ratio (0.69). However, the particle in a shell sample offered higher compliance therefore would be more suitable for use in the assembly of the actuator. This is summarized in the table below:

TABLE V. COMPARISON OF INDUCTANCE OF NON-VACUUMED FERROELASTOMER AND NON-VACUUMED PARTICLE IN A SHELL SAMPLE

Sample type	Particles sizes (microns)	Mean Inductance	Standard Deviation of Inductance
Ferroelastomer	100	793.98	17.849
Particle in a shell	100	791.02	18.39

The achieved relative permeability value is 5.2. Literature does not dictate the value of permeability beyond which flux begins to stray therefore this will be determined empirically from the sample fabricated.

Compliance characteristics:

TABLE VI. COMPLIANCE CHARACTERISTICS

Sample type	Particles sizes (microns)	Mean Inductance	Standard Deviation of Inductance	Compliance
Ferroelastomer	100	793.98	17.849	
Particle in a shell	100	791.02	18.39	

B. Soft Coil Measurements and Verification

In the fabrication of the coils, the first three prototypes lost their conductivity after being wound on the mold. The loss in conductivity is due to separation in the liquid metal alloy as a result of being stretched. However, before they lost their conductivity they were measured, and their electrical characteristics used to derive the conductivity of EGaIn as shown in table VII below. The average resistivity is 2.48×10^{-7} Ohm meters with a standard deviation of 4.7043×10^{-8} Ohm meters. Resistivity is the reciprocal of Conductivity: $\sigma = 4.03 \times 10^6 \text{ Sm}^{-1}$.

TABLE VII. SOFT WIRE CHARACTERIZATION

Tube diameter (mm)	EGaIn Length (m)	Electrode diameter	Electrode length (m)	Total Resistance (Ω)	Computed EGaIn resistivity ($\Omega \text{ m}$)
0.3	1.20	30 AWG (0.254 mm)	0.11	3.566	2.0791E-7
0.3	1.705	28 AWG (0.32004 mm)	0.14	5.74	2.368E-7
0.5	4	22 AWG (0.64516 mm)	0.073	6.115	2.999E-7

The fourth prototype successfully retained its conductivity because it was wound with less turns and less stress. The results are shown in the table below:

TABLE VIII. PROTOTYPE IV COIL CHARACTERISTICS

Tube diameter (mm)	EGaIn Length (m)	Electrode diameter	Electrode length (m)	Total R (Ω)	EGaIn resistivity ($\Omega \text{ m}$)	N	L uH
0.3	0.409	28 AWG (0.32004 mm)	0.17	1.413	2.38E-7	10	1.67

These values were then used to determine the electrical characteristics of a similar coil but with 30 turns i.e. (about 1 meter):

$$R = \frac{\rho \ell}{A} = 3.37 \Omega \approx 4 \Omega$$

$$L = \frac{\mu N^2 A}{\ell} = 9.99 \text{ uH} \approx 10 \text{ uH}$$

A simulation conducted with 4 Ω and 2uH reveals a voltage spike of about 170V when the capacitor discharges.
 ## explain impliations of 170 V on the amount of current

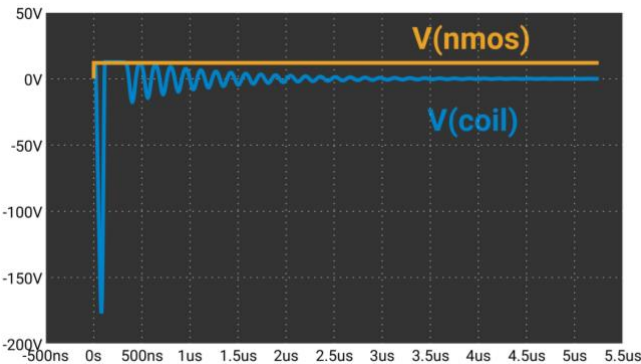


Fig. 41. Discharing capacitors on a coil model with 4 Ohms resistance and 2uH inductance.V(nmos) is the voltage of a signal used to switch a transistor connecting the coil to two 220uF capacitors.

Magnetic field strength characterization: A Gauss meter is used to determine the magnetic flux density of prototype IV. The setup involves connecting the coil to a current source and placing a gauss meter probe inside the coil to measure the flux (B). The field strength(H) is then calculated from the magnetic flux(B). Fig. 42 shows the plot of current vs magnetic field generated from the coil.

Fig. 42. Plot of magnetic flux of coil against amount of current flowing through the prototype IV coil.

Fig. 43. Setup for measuring the magnetic flux and magnetic field strength of the flexible coil

Transient current limit: Literature does not point to the amount of transient current that would cause an EGaIn conductor to fuse or structurally disintegrate. Therefore, this is determined empirically by taking a short EGaIn tube conductor of 100 mm length and sequentially passing a predetermined amount of current. A short conductor is necessary here so as to have an equivalently lower resistance and achieve higher transient currents. The transient current is driven through the wire for about 50 μ s then and the resistance measured. The objective is to determine whether high currents increment the resistance which would be a sign of structural damage.

Fig. 44. Plot of resistance of EGaIn tube conductor measured after driving a transient current across the conductor.

C. Soft magnetic core Measurement and Verification

Remanence: The flexible permanent magnets are magnetized in a pulse magnetizer and the residual magnetisms measured. The results are summarized in table IX. For the singular integrated bar prototype, the sample is first magnetized with a high force(2.7 T) to make sure that NdFeB is magnetized, then a smaller force is used to switch the polarity of AlNiCo. The results in table IX only show the residual magnetism with respect to the direction in which AlNiCo is magnetized to.

TABLE IX. RESIDUAL MAGNET FIELD OF FLEXIBLE PERMANENT MAGNETS		
Prototype	Pulse magnetizer setting (Tesla)	Remanence (Br) in Tesla
Flexible AlNiCo (separate bar)	2.7	
Flexible NdFeB (separate bar)	2.7	
Singular integrated bar (same direction)		
Singular integrated bar (opposite directions)		

Coercivity: The permanent magnets are characterized using a pulse magnetizer and a Gauss meter. A magnetic field is applied on each prototype at intervals of 0.3 T up to a maximum of 2.7 T. After each interval the residual magnetic field is measured. The results are plotted in the Fig. 45 and Fig. 46 for each prototype.

Fig. 45. Plot of the residual magnetic field of flexible AlNiCo (left) and flexible NdFeB (right) for the separate bar prototype.

Fig. 46. Plot of the residual magnetic field of the singular integrated bar prototype

D. Assembled device Measurement and Verificaiton

Length:

Holding Force:

Compliance:

Actuation performance: The soft EPM is tested against a rigid EPM to determine its latching performance on different geometric surfaces. The setup involves steel balls of different diameters and steel cubes of different dimensions summarized in table X and table XI. The EPMs are then latched onto the surface of each and the force needed to detach them measured using a string tied to a spring of known spring constant k .

TABLE X. SOFT EPM VS RIGID EPM PERFORMANCE ON A SPHERICAL TARGET SURFACE

<i>Diameter</i>	<i>Rigid EPM force (N)</i>	<i>Soft EPM force (N)</i>

TABLE XI. SOFT EPM VS RIGID EPM PERFORMANCE ON A CUBICAL TARGET SURFACE

<i>Dimension s(l x w x h in mm)</i>	<i>Rigid EPM force (N)</i>	<i>Soft EPM force (N)</i>

VII. BUDGET

A complete list of the purchased materials used in this project is attached in appendix ###. The objective of this project was to confirm the feasibility of a soft compliant EPM. Given its exploratory nature cost did not impose a significant constraint in the design phase. Table XII summarizes the minimum material requirements needed to reproduce a functioning prototype. However, this does not factor in the tools, machinery and measuring instruments used to fabricate the components.

TABLE XII. MINIMUM MATERIALS NEEDED TO FABRICATE A FLEXIBLE EPM

<i>Material</i>	<i>Quantity</i>	<i>Cost (USD)</i>

VIII. CONCLUSION AND FUTURE WORK

The objective in the project is to convert a rigid actuator into compliant one with higher compatibility for soft robotics and higher surface adaptation characteristics. Such a device can be used in self assembling robotic systems by embedding them in joints, robots that have to navigate over metallic surfaces. The results in the measurement section suggest the feasibility of such a flexible actuator.

A. Summary of Achieved Technical Specifications

The table below summarizes the achieved values with regards to the technical specifications:

TABLE XIII. SUMMARY OF TECHNICAL SPECIFICATIONS

<i>Specification</i>	<i>Target value</i>	<i>Achieved value</i>
Device Scale	1 cm long	
Holding Force	2 N	
Soft Iron End relative permeability	10	5.2
Soft Iron End compliance	0.001 to 0.05 GPa	
Hard Permanent Magnet coercivity	1000 kA/m	
Semi-hard Permanent coercivity	50 kA/m	
Semi-hard Permanent magnet compliance	0.001 to 0.05 GPa	
Coil conductivity	$3.4 \times 10^6 \text{ Sm}^{-1}$	$4.03 \times 10^6 \text{ Sm}^{-1}$
Coil magnetic field strength	100 kA/m	
Coil transient current limit	20 A	

B. Future Work

Given that most of the parts were fabricated out of Ecoflex the potential of adapting the device design geometries to suite custom robots is unbound. A future version would involve the use of a 3D printer to dispense mixed materials and extrude a desired shape, or the use of specialized molds to embed EPMs directly into soft robotic systems. Specialized fabrication methods such as the latter and former would allow for the production of a device at an even smaller scale which would have the advantage of exerting greater force.

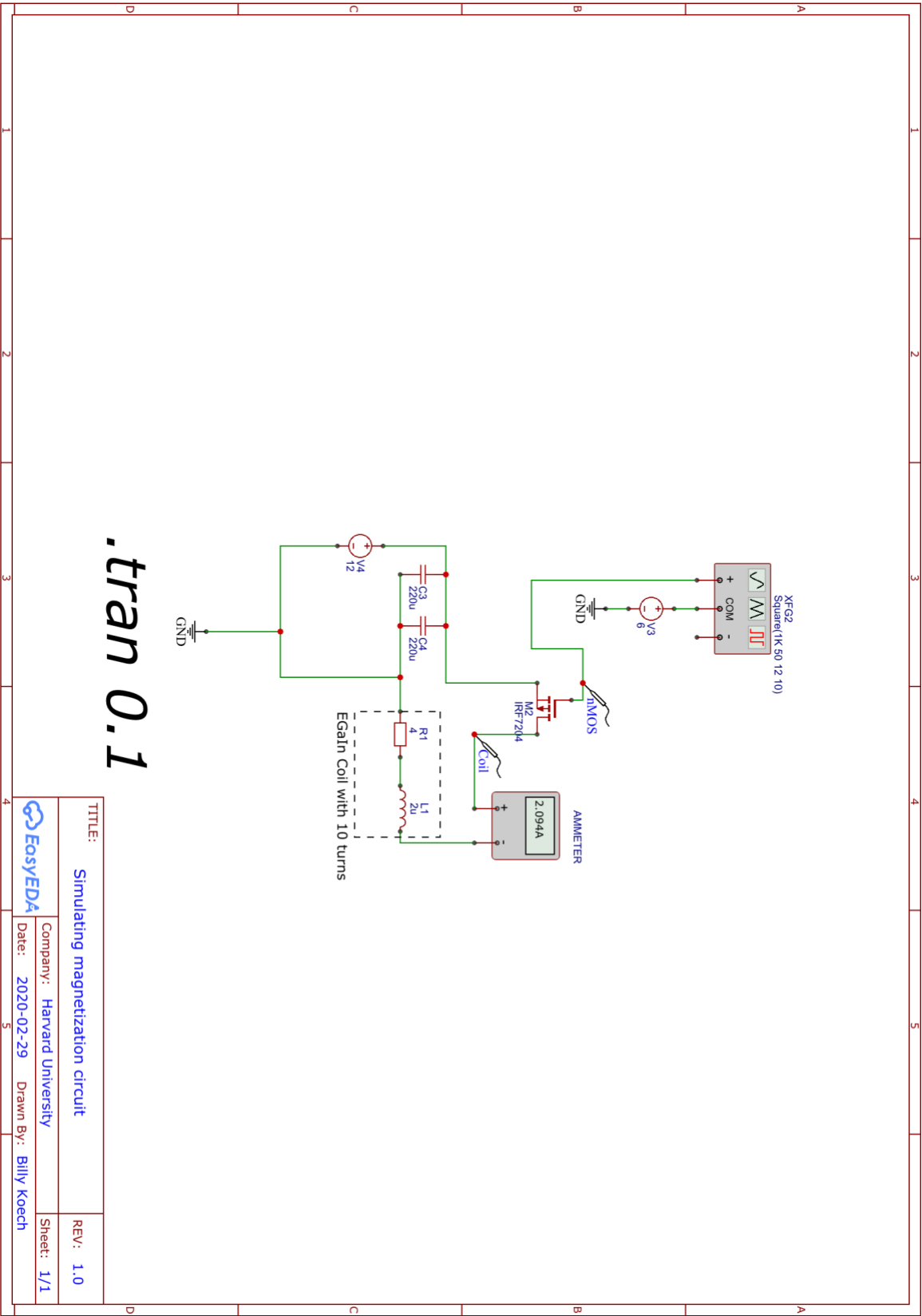
ACKNOWLEDGMENT

The author gratefully acknowledges the contribution of Bahar Haghighat, Radhika Nagpal, Anas Challar, Daniel Prendergast, the active leaning labs(ALL) staff and the ES100 staff for their guidance and support throughout the project.

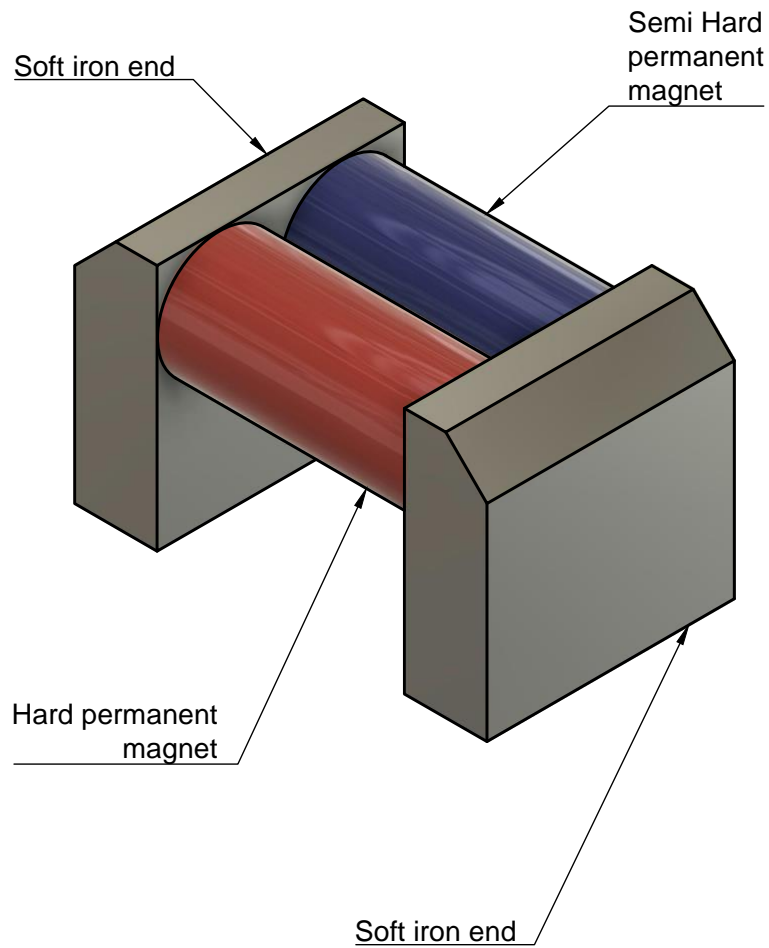
REFERENCES

- [1] F. Ilievski, A. D. Mazzeo, R. F. Shepherd, X. Chen, and G. M. Whitesides, "Soft Robotics for Chemists," *Angewandte Chemie International Edition*, vol. 50, no. 8, pp. 1890–1895, 2011, doi: 10.1002/anie.201006464.
- [2] "Challenges and Opportunities for Design, Simulation, and Fabrication of Soft Robots | Soft Robotics." [Online]. Available: <https://www.liebertpub.com/doi/abs/10.1089/soro.2013.0007>. [Accessed: 02-Oct-2019].
- [3] P. Boyraz, G. Runge, and A. Raatz, "An Overview of Novel Actuators for Soft Robotics," *Actuators*, vol. 7, no. 3, p. 48, Sep. 2018, doi: 10.3390/act7030048.
- [4] A. N. (Ara N. Knaian, "Electropermanent magnetic connectors and actuators : devices and their application in

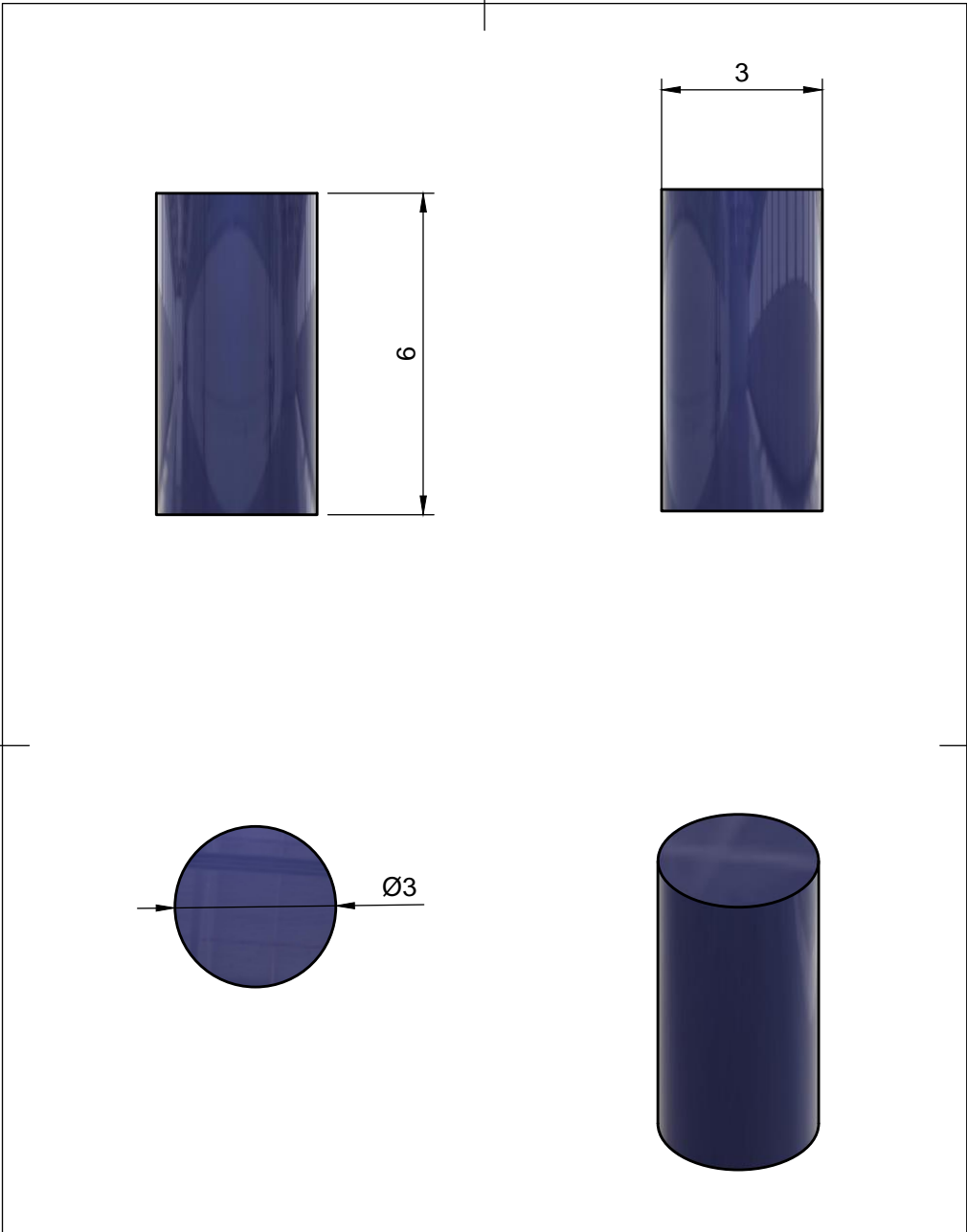
- programmable matter,” Thesis, Massachusetts Institute of Technology, 2010.
- [5] R. Guo, L. Sheng, H. Gong, and J. Liu, “Liquid metal spiral coil enabled soft electromagnetic actuator,” *Sci. China Technol. Sci.*, vol. 61, no. 4, pp. 516–521, Apr. 2018, doi: 10.1007/s11431-017-9063-2.
 - [6] M. Raad, “Miniature Electro-Permanent Magnets for Modular Soft Robots.”
 - [7] B. Haghighat, E. Droz, and A. Martinoli, “Lily: A miniature floating robotic platform for programmable stochastic self-assembly,” in *2015 IEEE International Conference on Robotics and Automation (ICRA)*, 2015, pp. 1941–1948, doi: 10.1109/ICRA.2015.7139452.
 - [8] “Miniature Soft Electromagnetic Actuators for Robotic Applications - Do - 2018 - Advanced Functional Materials - Wiley Online Library.” [Online]. Available: <https://onlinelibrary.wiley.com/doi/abs/10.1002/adfm.201800244>. [Accessed: 04-Oct-2019].
 - [9] “Micrometals Powder Core Solutions.” [Online]. Available: <https://micrometals.com/materials/pc>. [Accessed: 01-Mar-2020].
 - [10] “MAGNETISM.eu - EMA - The European Magnetism Association.” [Online]. Available: <http://magnetism.eu/>. [Accessed: 04-Oct-2019].
 - [11] “Physics - Young’s modulus - University of Birmingham.” [Online]. Available: <https://www.birmingham.ac.uk/undergraduate/preparing-for-university/stem/Physics/stem-legacy-Youngs-modulus.aspx>. [Accessed: 06-Oct-2019].
 - [12] G. Bai, R. W. Gao, Y. Sun, G. B. Han, and B. Wang, “Study of high-coercivity sintered NdFeB magnets,” *Journal of Magnetism and Magnetic Materials*, vol. 308, no. 1, pp. 20–23, Jan. 2007, doi: 10.1016/j.jmmm.2006.04.029.
 - [13] P. Campbell and S. Al-Murshid, “A model of anisotropic Alnico magnets for field computation,” *IEEE Transactions on Magnetics*, vol. 18, no. 3, pp. 898–904, May 1982, doi: 10.1109/TMAG.1982.1061943.
 - [14] G. J. Hayes, Ju-Hee So, A. Qusba, M. D. Dickey, and G. Lazzi, “Flexible Liquid Metal Alloy (EGaIn) Microstrip Patch Antenna,” *IEEE Trans. Antennas Propagat.*, vol. 60, no. 5, pp. 2151–2156, May 2012, doi: 10.1109/TAP.2012.2189698.
 - [15] “GitHub - kimkoech/ferroelastomer_property_analysis: Analysis of the permeability and compliance of different mixtures of iron and elastomers.” [Online]. Available: https://github.com/kimkoech/ferroelastomer_property_analysis. [Accessed: 01-Mar-2020].



APPENDIX II – EPM Assembly (Isometric projection)

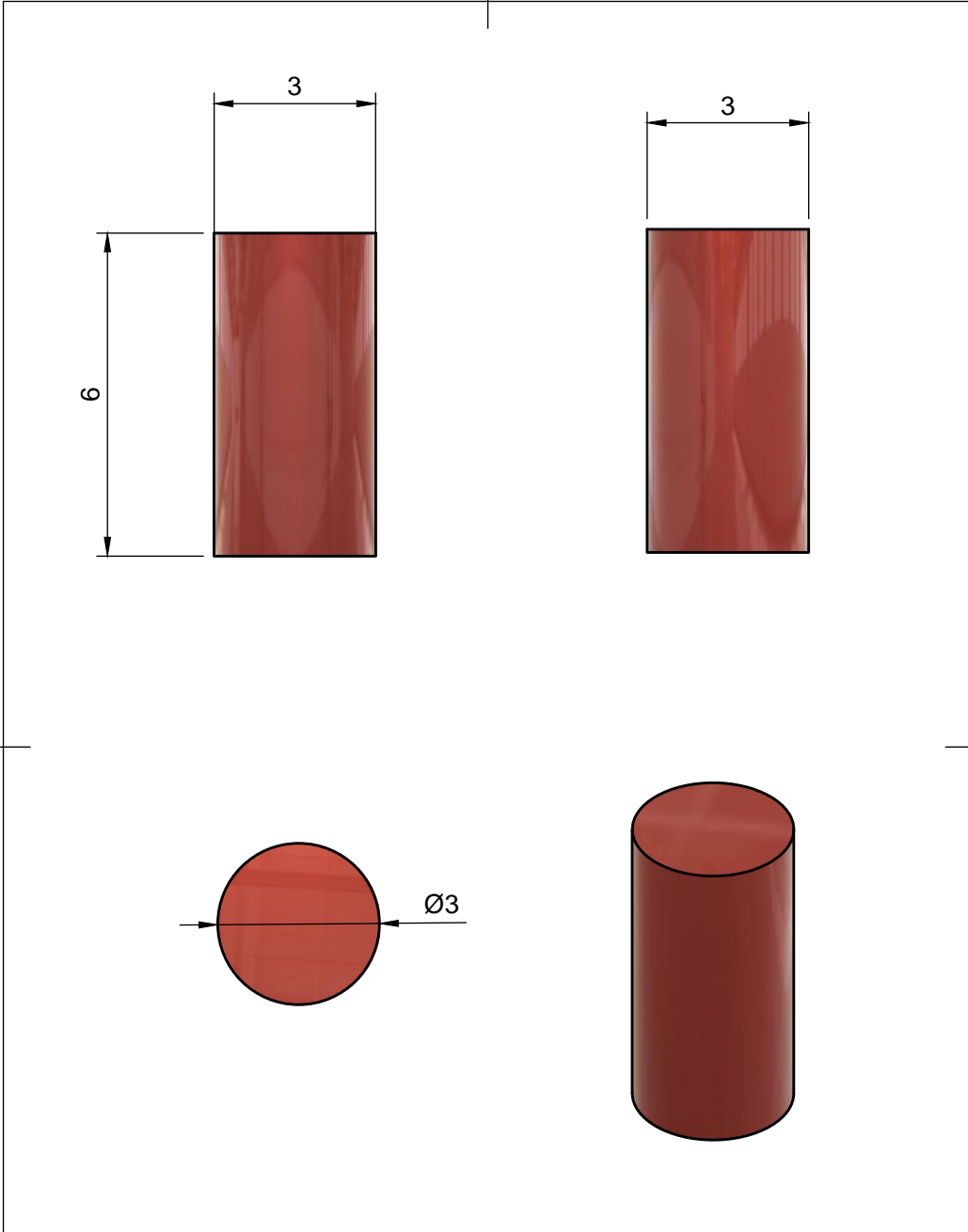


Dept.	Technical reference	Created by Billy Koech	11/6/19	Approved by
		Document type	Document status	
		Title EPM Assembly	DWG No.	
		Rev.	Date of issue	Sheet 1/1



Dept.	Technical reference	Created by Billy Koech	11/6/19	Approved by
		Document type	Document status	
		Title Semi-Hard Permanent Magnet	DWG No.	
			Rev.	Date of issue
			Sheet	1/1

APPENDIX IV – Hard permanent magnet

			
Dept.	Technical reference	Created by Billy Koech	Approved by 11/6/19
		Document type	Document status
		Title Hard Permanent Magnet	
		DWG No.	
		Rev.	Date of issue
		Sheet 1/1	

APPENDIX V - Inductance of fabricated samples using Ecoflex 30

<i>Sample number</i>	<i>Volume Ratio</i>	<i>Particle size in microns</i>	<i>Mass ratio</i>	<i>Ecoflex type</i>	<i>Vacuumed?</i>	<i>Average inductance in uH</i>	<i>Standard deviation of inductance</i>	<i>Median inductance in uH</i>
1	0.09615385	210	0.25696594	30	0	443	5.90550591	442.9
2	0.27272727	210	0.57803762	30	0	529.02	34.4605862	525.9
3	0.38461538	210	0.68006008	30	0	590.32	21.9175044	580.7
4	0.5	210	0.77412399	30	0	689.74	4.66936827	686.9
5	0.6	210	0.84102268	30	0	786.38	20.4585434	790.1
6	0.63636364	210	0.86850153	30	0	845.1	12.6200238	844.4
7	0.11111111	100	0.27868852	30	0	461.24	2.12202733	460
8	0.33333333	100	0.56903353	30	0	607.3	7.80224327	606.9
9	0.5	100	0.74321985	30	0	736.6	9.68090905	734.2
10	0.6	100	0.81024989	30	0	790.72	20.7183976	782.6
11	0.66666667	100	0.83388218	30	0	811.84	6.50676571	812.5
12	0.69230769	100	0.8538961	30	0	793.98	17.849986	790
13	0.11111111	300	0.21052632	30	0	466.34	7.58142467	465.6
14	0.33333333	300	0.44880952	30	0	609.4	3.89679355	610.1
15	0.5	300	0.58854626	30	0	699.54	13.4988148	703.2
16	0.6	300	0.67280453	30	0	717.02	13.2861582	723.4
17	0.66666667	300	0.72754313	30	0	768.4	12.4925978	761.6
18	0.69230769	300	0.74704619	30	0	767.88	18.4552702	763.2
19	0.5	300	0.56962025	30	2	629.16	6.01564627	627.1
20	0.11111111	6	0.19	30	0	455.02	0.94180677	454.9
21	0.33333333	6	0.48813559	30	0	498.56	1.44499135	498.5
22	0.5	6	0.71965318	30	0	596.86	7.01305925	600.2
23	0.6	6	0.79161028	30	0	679.32	6.98333731	683.4
24	0.66666667	6	0.81055156	30	0	714.46	8.8429633	718.7
25	0.69230769	6	0.84712111	30	0	727	10.6400188	734.2
26	0.11111111	1-4	0.22259136	30	0	442.04	0.62289646	441.8
27	0.33333333	1-4	0.54356061	30	0	497.94	1.225969	498
32	0.11111111	100	0.34146341	30	0	507.44	0.68774995	507.6
33	0.69230769	100	0.85378835	30	0	787.42	9.5470938	788.3
34	0.11111111	210	0.3615495	20	0	482.68	3.22753776	482.7
35	0.33333333	210	0.65570008	20	0	633.5	0.86890736	633.4
40	0.11111111	210	0.4596577	30	0	502.18	9.93614613	502.5
41	0.33333333	210	0.65245374	30	0	618.82	7.47810136	620.1
42	0.5	210	0.78998073	30	0	705.38	19.6643586	703.6
43	0.6	210	0.83777068	30	0	751.38	7.43283257	754.5
44	0.66666667	210	0.79794118	30	0	786.38	5.30678811	784.8

APPENDIX V - Inductance of fabricated samples using Ecoflex 30

45	0.69230769	210	0.88229084	30	0	796.48	13.8591847	801.2
47	0.11111111	300	0.1352459	30	1	433.06	2.47749874	433
48	0.33333333	300	0.40684932	30	1	531.88	7.24548135	532.7
49	0.5	300	0.54771784	30	1	665.76	3.66851469	664.8
50	0.6	300	0.68828298	30	1	699.42	22.6114352	700.1
51	0.66666667	300	0.73511543	30	1	755.88	19.6403157	756.5
52	0.69230769	300	0.75447427	30	1	733.28	15.3002288	730.6

APPENDIX VI – Relative permeability of fabricated samples using Ecoflex 30

<i>Sample Number</i>	<i>Volume ratio</i>	<i>Particle size</i>	<i>Mass ratio</i>	<i>Ecoflex type</i>	<i>Vacuumed?</i>	<i>Average relative Permeability</i>	<i>Standard Deviation of relative permeability</i>	<i>Median of relative permeability</i>
1	0.09615385	210	0.25696594	30	0	2.78888975	0.03717789	2.78826021
2	0.27272727	210	0.57803762	30	0	3.33042541	0.21694532	3.31078357
3	0.38461538	210	0.68006008	30	0	3.71633724	0.13798082	3.6557749
4	0.5	210	0.77412399	30	0	4.34223209	0.02939583	4.32435298
5	0.6	210	0.84102268	30	0	4.95062556	0.12879599	4.97404468
6	0.63636364	210	0.86850153	30	0	5.3202951	0.07944888	5.31588828
7	0.11111111	100	0.27868852	30	0	2.90371898	0.01335914	2.89591261
8	0.33333333	100	0.56903353	30	0	3.82323419	0.04911873	3.82071601
9	0.5	100	0.74321985	30	0	4.63723745	0.0609458	4.62212834
10	0.6	100	0.81024989	30	0	4.97794787	0.13043189	4.92682871
11	0.66666667	100	0.83388218	30	0	5.11090803	0.0409631	5.11506303
12	0.69230769	100	0.8538961	30	0	4.99847107	0.11237391	4.97341513
13	0.11111111	300	0.21052632	30	0	2.93582584	0.04772857	2.9311672
14	0.33333333	300	0.44880952	30	0	3.83645466	0.02453212	3.84086148
15	0.5	300	0.58854626	30	0	4.40392762	0.08498128	4.42696901
16	0.6	300	0.67280453	30	0	4.5139723	0.08364251	4.55413735
17	0.66666667	300	0.72754313	30	0	4.83743315	0.07864668	4.79462401
18	0.69230769	300	0.74704619	30	0	4.83415951	0.11618446	4.80469675
19	0.5	300	0.56962025	30	2	3.96085299	0.03787127	3.94788434
20	0.11111111	6	0.19	30	0	2.86456121	0.00592911	2.86380575
21	0.33333333	6	0.48813559	30	0	3.13866563	0.00909689	3.1382879
22	0.5	6	0.71965318	30	0	3.75750956	0.04415045	3.77853641
23	0.6	6	0.79161028	30	0	4.27663338	0.04396334	4.30231886
24	0.66666667	6	0.81055156	30	0	4.49785592	0.05567054	4.52454868
25	0.69230769	6	0.84712111	30	0	4.57680101	0.06698384	4.62212834
26	0.11111111	4-Jan	0.22259136	30	0	2.78284611	0.00392142	2.7813352
27	0.33333333	4-Jan	0.54356061	30	0	3.13476244	0.00771804	3.13514017
32	0.11111111	100	0.34146341	30	0	3.19456934	0.0043297	3.19557661
33	0.69230769	100	0.85378835	30	0	4.95717284	0.06010337	4.96271285
34	0.11111111	210	0.3615495	20	0	3.03869369	0.02031884	3.0388196
35	0.33333333	210	0.65570008	20	0	3.9881753	0.00547017	3.98754575
40	0.11111111	210	0.4596577	30	0	3.1614552	0.06255263	3.16346975
41	0.33333333	210	0.65245374	30	0	3.89575791	0.0470781	3.90381611
42	0.5	210	0.78998073	30	0	4.44069312	0.12379623	4.4294872
43	0.6	210	0.83777068	30	0	4.73028438	0.04679312	4.74992622

APPENDIX VI – Relative permeability of fabricated samples using Ecoflex 30

44	0.66666667	210	0.79794118	30	0	4.95062556	0.03340868	4.94067873
45	0.69230769	210	0.88229084	30	0	5.01420973	0.08724997	5.04392431
47	0.11111111	300	0.1352459	30	1	2.72631286	0.015597	2.72593513
48	0.33333333	300	0.40684932	30	1	3.34843043	0.04561365	3.35359271
49	0.5	300	0.54771784	30	1	4.19126691	0.023095	4.18522327
50	0.6	300	0.68828298	30	1	4.40317217	0.14234944	4.40745308
51	0.66666667	300	0.73511543	30	1	4.75861396	0.12364486	4.76251715
52	0.69230769	300	0.75447427	30	1	4.61633652	0.09632201	4.59946468

APPENDIX VII - Budget

BOM (Bill of Materials)	Unit Cost \$	Unit	# of Units	Total \$
Item	\$ 5.00	20 pack	1	\$ 5.00
Ecoflex 10, 20, 30				
Soft iron particles				
Hard magnetic particles (250mg)	\$4.85			
Semi hard magnetic particles (1kg)	\$20			
Silver nano wires	\$423			
Eutectic Gallium Indium(10g)	\$118			

Please do your best to fill in the following details on your budget	Total \$		Exact or estimated?
Total Development cost: everything that was spent on your project including prototypes, transportation to research locations, renting of equipment, orders from a lab you worked at, your own money etc...?etc...			
What is the minimum cost to make one prototype of your project (\$0 is an option)?			
Total cost of items purchased through the Active Learning Labs (ALL), if any			
Total cost covered by the Harvard Research Lab(s) you are affiliated with, if any			
Total cost of items purchase personally, if any			
Total cost covered by a non-Harvard lab and/or company, if any			